Asian Journal of Physics
Vol. 31, No 2 (2022) 365-373
Available on: www.asianjournalofphysics.com

ap

Bromide hydration as a function of concentration and temperature

Letizia Scarabattoli[1], Lucia Comez[2] and Paola Sassi[1*]

[1]*Department of Chemistry, Biology and Biotechnology, University of Perugia, Via Elce di sotto 8, 06123 Perugia, Italy*

[2]*CNR-IOM, c/o Department of Physics and Geology, University of Perugia, Via Pascoli, 06123 Perugia, Italy*

In the fascinating world of the physico-chemical properties of water vibrational spectroscopy provides a powerful tool to unravel the complicated scenario of H-bonding structures. In this work, we used Raman spectroscopy to give an estimate of interactions and nearest-neighbour distances in water and KBr aqueous solutions. By H/D isotopic substitution and analysis of the OH/OD stretching regions, we followed the rearrangement of local structures in the proximity of bromide ions as a function of temperature, in the –30°C - 50°C temperature range, at different KBr concentrations. A more compact and interacting shell was recognized for the solution in the presence of ice, regardless of KBr concentration; however, both at high and low temperatures, a 20% lessening of H bonding enthalpy was estimated in water-bromide with respect to water-water interactions. This analysis of water properties in the bromide hydration shell below and above the melting range, gives a more comprehensive picture of the H bond network of water-electrolyte systems.

Keywords: Water, Electrolyte, Hydration, Raman spectroscopy.

1 Introduction

Water in nature is one of the main constituents of ecosystems and is necessary to all known forms of life. Liquid water is one of the most studied systems, but at the same time, it is most difficult to fully understand due to its peculiar physico-chemical characteristics [1-3]. In the condensed phases, many of the properties of H_2O are due to the presence of hydrogen bonds between neighboring molecules, to form a network that extends over the entire volume [4]. With respect to the solid phase, the liquid water is characterized by the absence of long-range order and in a lower average hydrogen bond (HB) strength [5]. Due to the ice structure, the difficulty to represent the variety of H-bonded species, different structural models have been postulated for liquid water. Many of these models describe liquid water as an equilibrium of discrete molecular structures characterized by a different number of hydrogen bonds per molecule and/or a different geometry of HB clusters [6-8]. Each water molecule can act as double accepting and double donating HB unit in the local pentamer structure; the irregular distortions and elongations of local tetrahedral arrangements are expected to be higher in the liquid than in the solid phase, and to increase with increasing temperature. To study the properties of HB strength and HB structures, vibrational spectroscopy, and particularly Raman spectroscopy, comes to our aid, since the vibrational signals are highly sensitive to the strength and extension of this interaction [9].

Salts of monatomic ions in water dissociate into cations and anions, which interact with the H_2O molecules and orient them. Around each ion, a certain number of water molecules (hydration number) is present and is greater the larger the size of the ion itself [10]. These water molecules interact with the ion

Corresponding author
e mail: paola.sassi@unipg.it (Paola Sassi)

through hydrogen bonds and form the hydration shell. Naturally, the water molecules surrounding the cation behave as acceptors, while those in the hydration shell of the anion will act as hydrogen bonding donors. Depending on the type and concentration of the electrolyte, higher solvation shells may also be considered consisting of water molecules that are affected by the influence of the ion, but which are not directly linked to it. Regarding the extension of hydration shell, it is difficult to define it exhaustively: we call hydration shell the ensemble of water molecules with properties different from pure water, thus it strongly depends on the properties that are probed, and therefore by the technique used to study the solution structure [11].

The ion induces a new local order and a different restructuring capacity in the solution compared to bulk water, by accepting or donating H-bonds. The ions that interact weakly with water increase the disorder and weaken the hydrogen bond, while the ions that interact strongly impose greater local order on the water molecules that surround them. Small ions, can locally create a condition of order and a high local density; large single-charge ions behave like hydrophobic molecules, increasing the disorder. This restructuring at a microscopic level also affects the macroscopic properties of the water, including viscosity [12]. The effects are different depending on the type of ion, charge and size. [13,14]

Vibrational spectroscopy techniques have made it possible to observe that as the concentration of the salt increases, the water-anion interaction significantly changes the characteristic signals of water, while the effect of the cation is much less evident [15].

In this work, we characterize the properties of the water molecules in the bromide hydration shell, taking a simple electrolyte, KBr, as a casus studii. To characterize the hydration properties, we used vibrational Raman spectroscopy because it is very informative about the structure and dynamics of hydrogen bonding systems [16-18]. Many theoretical and experimental studies [19-23] have been made over the years to understand the properties of water in the ion/solute hydration shell, most of them at room temperature. In the present study, we analyzed KBr solutions in a wide range of temperatures, including below the melting temperature, to describe the perturbation of HB network. Frozen electrolytic solutions are of fundamental importance in the geochemical and astrochemical fields [24-26]; therefore, we used Raman spectroscopy to characterize the hydration shell for bromide solutions in the presence of ice to mimic situations similar to those under extreme conditions.

2 Materials and Methods

KBr was purchased from Riedel-de Haën with purity of 99%. KBr solutions were prepared by weight, in salt/water mole ratio 1/39 (diluted solution, hereafter KBr dil) and 1/8 (concentrated solution, hereafter KBr conc). The solutions at the same KBr concentration were prepared in a 50% H_2O/D_2O mixture. D_2O was purchased from Sigma-Aldrich and used as such without further purification. Ultrapure water (resistivity: 18.2 MX/cm at 298 K) was obtained with a Millipore Direct-Q–3 UV purification system.

Raman measurements were performed using a solid-state laser OXXIUS mod. LMX-532S-300 emitting at 532 nm with a 300 mW power radiation. All the Raman spectra were collected in backscattering configuration and the radiation was analyzed by the monochromator Horiba *i*HR320, and revealed by the CCD Horiba mod. Syncerity. The spectra were recorded in the 1100-4200 cm^{-1} region as the average of 30 scans, 10 seconds each, with a resolution of 3 cm^{-1}. A Linkam Stage FTIR600 was used as a temperature control system: the cell with the sample inside was slowly cooled (cooling rate 2°C/min) down to –30°C, left at this temperature for 30 minutes and then heated up to 50°C at 1°C/min. Spectra were recorded every 2°C with a step-scan acquisition (constant temperature during spectrum acquisition then heating at 1°C/min), in a range, –30°C - 50°C. The polarizations of incident and scattered radiations were selected to be parallel (VV configuration) ; the resulting spectra were baseline-corrected using the Labspec6 software from Horiba. At the salt concentrations here studied, at low temperatures a two-phase system was obtained, with pure ice separating from a KBr solution [27].

To isolate the spectral contribution of hydration water both above and below the melting temperature, bulk-free Raman (BF-Raman) spectra were obtained by the difference between the spectrum of KBr solutions and the rescaled spectrum of the corresponding solvent, as described elsewhere [28]; the rescaling factor was determined to give the maximum non-negative spectral profile.

3 Result and Discussion

The OH stretching signals of liquid water and ice, respectively at 25°C and –30°C, are shown in Fig 1. It is well known that this band is a good probe of the H-bonding interactions in the liquid and solid systems since the stronger this interaction the lower is the OH-stretching frequency [29]. The Raman spectrum of ice shows an intense peak at about 3140 cm^{-1}: this is due to vibrations of OH oscillators engaged in ideal tetrahedral hydrogen bond configurations of the Ih solid structure. This spectral component has a similar counterpart in the OH stretching profile of liquid water; in fact, liquid water maintains a short range tetrahedral arrangement similar to the one that is present in ice, and the sub-band at around 3200 cm^{-1} of the OH-stretching profile of the liquid is assigned to these ice-like structures. Two other components are present in the ice spectrum at approximately 3260 and 3360 cm^{-1}. According to the assignments reported in the literature by Hu and others [30], they are respectively related to water molecules that are in deformed tetrahedral hydrogen bond configurations and in single donor hydrogen bond (weakly bonded) configurations. Also, the profile of liquid water shows two high frequency sub-bands at ca. 3420 and 3600 cm^{-1}, that can be ascribed to the same structures [31].

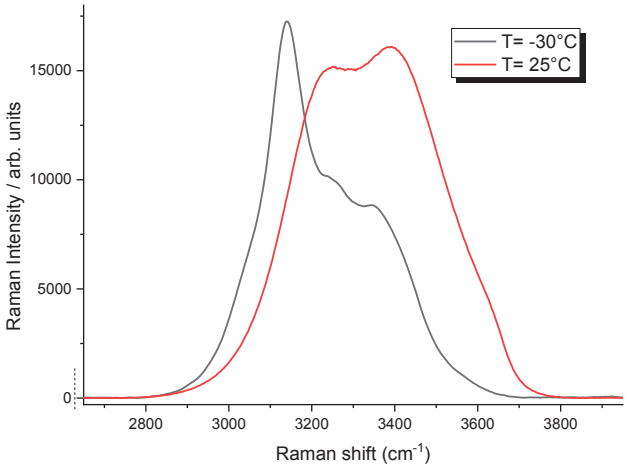

Fig 1. Raman spectra of ice and liquid water (polarized VV profile).

Figure 2 shows the OH stretching profiles of water and of diluted and concentrated KBr solutions at 25 ° C. Due to the addition of salt, the band maximum shifts to higher frequencies and undergoes a variation in the relative intensity of the three components described above. The blue shift indicates a weakening of the average strength of the hydrogen bond [32], passing from pure water to the more concentrated solution, and this is in line with previous experimental results [33]. The different band-shape is related to the different intensities of the 3260, 3420 and 3600 cm^{-1} contributions, which are further altered by the temperature variation.

As the temperature increases, a decrease in the intensity of the component at lower frequencies is observed in favor of the intermediate one, both for pure water and for the diluted KBr solution: this indicates a decrease in “ordered” and strongly bonded water structures, while the fraction of “disordered” water increases. The effect of increasing temperature is very similar to the one following the addition of KBr.

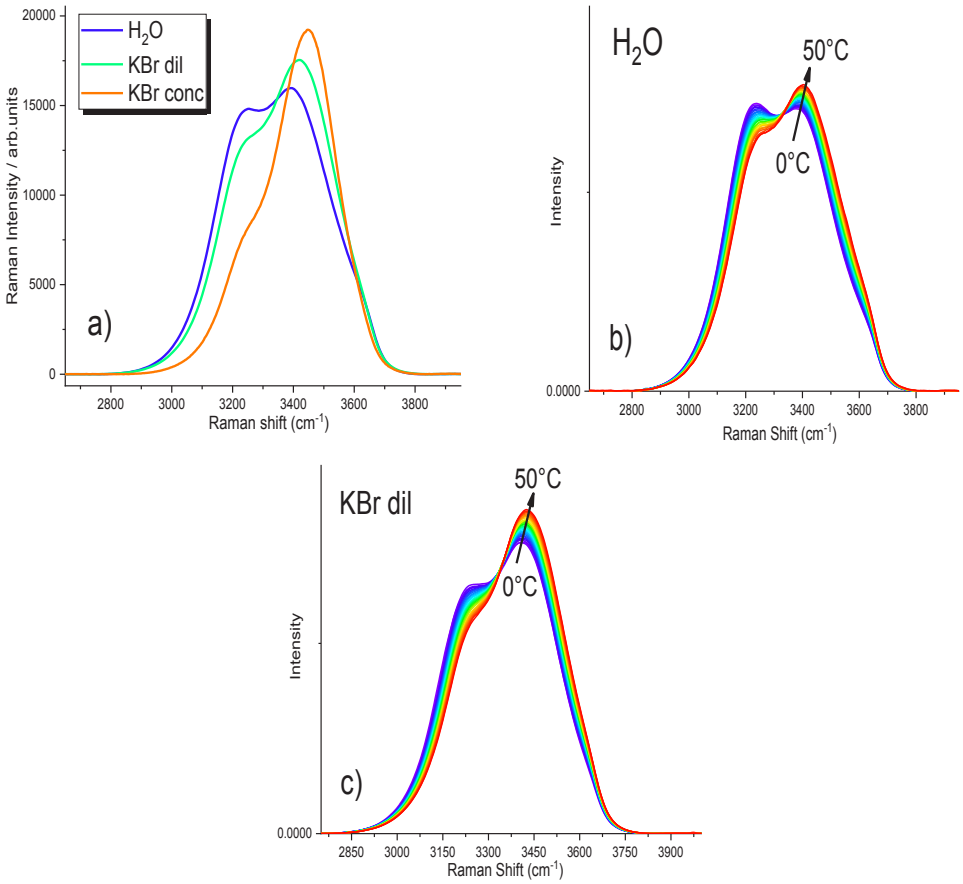

Fig 2. (a) Room temperature Raman spectra as a function of KBr concentration. (b) VV configuration Raman profile as a function of temperature for H_2O and (c) the dilute KBr solution.

The shift at higher frequencies observed by increasing temperature or KBr concentration is best appreciated by referring to the first moment, M_1, of the OH stretching band: this quantity estimates the average frequency of oscillators associated with the asymmetric profile, and was calculated using the equation:

$$M_1 = \frac{\int_{band} I(\nu)\ \nu\ d\nu}{\int_{band} I(\nu)\ d\nu} \tag{1}$$

where $I(\nu)$ is the scattering intensity at Raman shift, and integration is over the 2750-3850 cm^{-1} interval. Isotope substitution promotes the formation of distorted hydrogen bond configurations, due to an increase in hydrogen bond asymmetry in the presence of D_2O since hydrogen bonds in liquid D_2O are more linear and stronger than those in H_2O [30,34]. When D_2O is added to H_2O, the tetrahedral HB configurations are distorted, and the ordered water component has a very low intensity compared to H_2O [35] (Fig 3).

We used an equimolar H_2O/D_2O isotopic mixture as a solvent in order to reduce the intra- and intermolecular vibrational coupling on OH stretching profile and have a better probe of H-bonding interactions in KBr solution with respect to the pure solvent [34,36].

For both the OD and OH stretching signals, the blue-shift on increasing temperature can be observed, thus suggesting that a progressive rearrangement of the HB structures is observed in water and KBr solution on increasing temperature.

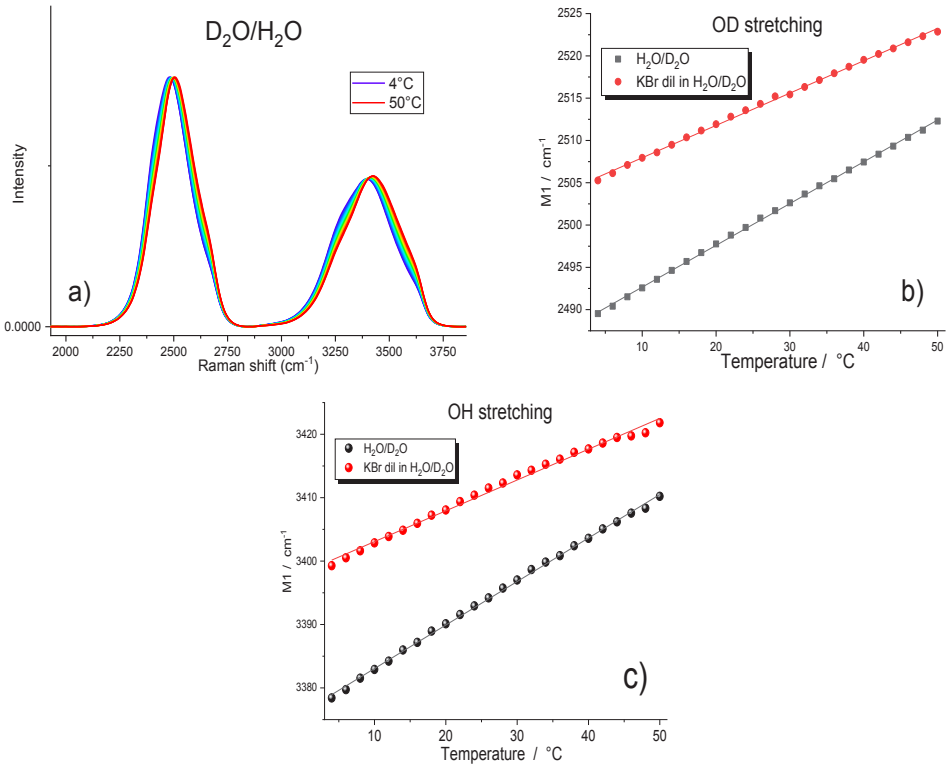

Fig 3. (a) OH and OD stretching profiles (VV configuration) of the equimolar D_2O/H_2O mixture, in the 4°C-50°C range. Dilute KBr solution and pure solvent: (b) temperature dependence of the first moment M_1 of OD stretching band; (c) temperature dependence of the first moment M_1 of OH stretching band.

Moreover, the vibrational frequency distributions associated with the two oscillators show that M_1 values increase in the solution compared to the pure solvent and that the temperature coefficient (slope of black and red lines in Fig 3(b) and 3(c) is lower in the presence of KBr. Higher M_1 values and lower temperature coefficients of the solution with respect to the pure solvent are agent related to the presence of ion-water HB interactions that are weaker than water-water ones. According to Smiechowski *et al* [36], the frequency of the OD stretching vibration can be used to estimate the average distances $R_{O..O}$ (Å) between water molecules. Using Eq (2), it is possible to calculate the nearest-neighbors oxygen-oxygen distance $R_{O..O}$ for the different systems:

$$\nu_{OD} = 2727 - \exp[16.01 - 3.73(R_{O..O})] \quad (2)$$

The $R_{O..O}$ values obtained for the different systems at room temperature and in the presence of ice are reported in Table 1.

Table 1. First moment of OD stretching band and average oxygen-oxygen distance

Sample	ν_{OD} (cm^{-1}) T = 25°C	$R_{O..O}$ (Å) T = 25°C	ν_{OD} (cm^{-1}) T= –30°C	$R_{O..O}$ (Å) T= –30°C
H_2O/D_2O	2500 ± 5	2.84 ± 0.01	2421± 5	2.76 ± 0.01
KBr dil	2513 ± 5	2.85± 0.01	(2421± 5)*	(2.76 ± 0.01)*
KBr conc	2540 ± 5	2.89± 0.01	(2420± 5)*	(2.76 ± 0.01)*

*: the strong intensity of ice signals probably hides the contribution from KBr solution

The $R_{O..O}$ distance increases in liquid KBr solutions with respect to pure water and the variation is small but progressive as the KBr concentration increases. The values found at room and low temperatures are compatible with those of the literature [37], but the strong intensity of ice signals probably hides the contribution of the solution to the spectrum.

To isolate the contribution of hydration water from the spectrum of the bulk, we applied the spectrum-subtraction procedure described in the experimental section. In Fig 4, the results of this subtraction (bulk-free BF Raman spectra) are compared to the profiles of neat water at 25°C and –30°C ($T = –30$°C is chosen as a reference of the system condition below the melting range). At both temperatures the position of band maximum is shifted to higher values in BF spectra with respect to the solvent; in addition, the low temperature data are red-shifted from those at room temperature.

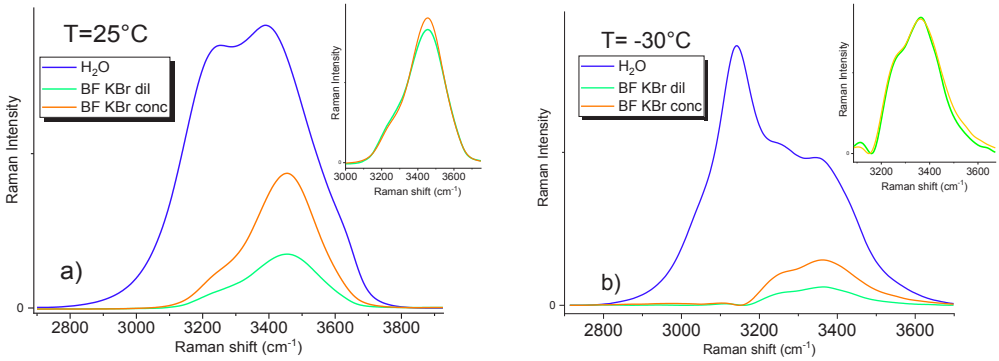

Fig 4. Bulk and bulk-free (BF) Raman spectra in the OH stretching region at 25°C (a) and –30°C (b). Normalized BF spectra of dilute and concentrated KBr solutions at 25°C and –30°C are shown in the insets of a) and b) panels, respectively.

At 25°C and –30°C BF profiles show similar band-shapes for both KBr solutions (see insets of Fig 4), indicating the same hydrogen bond interactions in the anion hydration shell as a function of concentration of KBr. In the H_2O/D_2O solvent, we also obtained similar results: we observed that the bandshape of BF profiles is not affected by the KBr concentration, both at 25°C and –30°C. In Table 2 the first moment of OH stretching signals of BF and pure solvent spectra are reported at the two temperatures.

Table 2. First moment of OH stretching band and average HB interaction strength

Sample	$T = 25$°C			$T = –30$°C		
	$M_1\ \nu_{OH}$ (cm^{-1})	$\Delta\bar{\nu}_{OH}$ (cm^{-1})	ΔH (kJ mol^{-1})	$M_1\ \nu_{OH}$ (cm^{-1})	$\Delta\bar{\nu}_{OH}$ (cm^{-1})	ΔH (kJ mol^{-1})
pure solvent*	**3396 ± 10**	274	21.2 ± 0.5	**3285 ± 10**	385	25.7 ± 0.4
BF KBr dil**	**3455 ± 20**	215	18 ± 1	**3325 ± 20**	345	24.2 ± 0.8
BF KBr conc**	**3466 ± 20**	204	18 ± 1	**3338 ± 20**	332	23.7 ± 0.8

*: H_2O/D_2O; **: H_2O/D_2O solutions

These average stretching frequencies (M_1 values) allow estimating an average strength of HB interaction (ΔH) from the well-known Badger-Bauer rule [38]. This correlation between the OH stretching frequency (ν_{OH}) and the strength of HB interaction ΔH is found in the literature in different forms; an extension of the classic Badger and Bauer rule has been proposed by Iogansen [39]:

$$\Delta H^2 = 1.92 \cdot (\Delta\bar{\nu}_{OH} - 40) \quad (3)$$

where, $\Delta\bar{\nu}_{OH} = \bar{\nu}_{OH} - \bar{\nu}_{OHf}$, is the frequency shift for the H-bonded species with respect to the free hydroxyl and ν_{OHf} is the OH stretching frequency for the free hydroxyl.

From the frequency of OH stretching band, we obtain that both in the liquid phase and at low temperatures, the water-ion interaction is lowered by about 18% compared to the water-water interaction. Besides, the M_1 values of OD stretching band of BF spectra can be used to evaluate the average oxygen-bromide distance $R_{O...Br-}$ according to Mikenda and Steinböch [40]:

$$\nu_{OD} = 2727 - 1.49 \cdot 10^6 \cdot \exp\left[-2.64(R_{O...Br-})\right] \quad (4)$$

Table 3. First moment of OD stretching band and average oxygen-bromide distance in the hydration shell

	$T = 25°C$		$T = -30°C$	
Sample	$M_1\ \nu_{OD}$ (cm^{-1})	$R_{O...Br-}$ (Å)	$M_1\ \nu_{OD}$ (cm^{-1})	$R_{O...Br-}$ (Å)
BF KBr dil*	2560 ± 20	3.45±0.04	2442 ± 20	3.24±0.03
BF KBr conc*	2549 ± 20	3.42±0.04	2425 ± 20	3.22±0.03

*: H_2O/D_2O solutions

Data of Tables 1- 3 give an exhaustive description of the structural properties of bromide aqueous solutions with respect to bulk water. In particular, the average water-anion distance is 3.44 (3.23) ± 0.03 Å in the liquid phase (below the melting range) which is higher than average water-water distance being 2.84 (2.76) ± 0.01 Å; this high intermolecular distance is related to the significant lowering in the strength of water-bromide with respect to water-water interaction.

5 Conclusions

In this work, the properties of electrolyte solutions were studied by Raman vibrational spectroscopy: in particular, aqueous solutions of KBr at different concentrations and as a function of temperature were analyzed.

The analysis of the OH stretching signal evidenced the weakening of the average hydrogen bond strength in the presence of KBr, respect to liquid water. Besides, we analyzed the hydration properties at temperatures below the melting range; also in the presence of ice, the high frequency component of OH stretching profile showed a higher intensity to suggest a lowering of the average HB interaction strength.

Bulk-free spectra were analyzed to isolate spectral contribution of the hydration shell from one of bulk water. Different BF spectra were obtained above and below the melting temperature: this allowed evaluating a different water-bromide distance and HB energy in the presence of ice with respect to the liquid phase, but, in both cases, a 20% lessning of HB interaction enthalpy was estimated. Interestingly, the same BF-Raman profile was obtained regardless of KBr concentration. This is probably due to our capability to monitor those water molecules directly interacting with bromide ion, which form the same first hydration shell both in the diluted and concentrated solution.

Our spectroscopic method could be further extended to the study of other binary salts to highlight their ability to modify the hydrogen bond network of water, and to study the extent of molecular-level distortions that solvation of ions causes in water and ice.

References

1. Shi R, Tanaka H, The anomalies and criticality of liquid water, *PNAS*, 117(2020)26591–26599.
2. Russo J, Tanaka H, Understanding water's anomalies with locally favoured structures, *Nat Commun*, 5(2014)3556; doi.org/10.1038/ncomms4556.

3. Bagchi B., Approaches to understand water anomalies, Water in Biological and Chemical Processes. From Structure and Dynamics to Function, (Cambridge university Press), (2013), pp 323–344.
4. Orgel L, The hydrogen bond, *Rev Mod Phys,* 31(1959)100–102.
5. Huang Y, Zhang X, Ma Z, Li W, Zhou Y, Zhou J, Zheng W, Sun C Q, Size, separation, structural order, and mass density of molecules packing in water and ice, *Sci Rep,* 3(2013)3005; doi.org/10.1038/srep03005.
6. Freda M, Piluso A, Santucci A, Sassi P, Transmittance FTIR spectra of liquid water in the whole Mid-infrared region: temperature dependence and structural analysis, *Appl Spectrosc*, 59(2005)1155–1159.
7. Gallina M E, Sassi P, Paolantoni M, Morresi A, Cataliotti R S, Vibrational analysis of molecular interactions in the aqueous glucose solutions. Temperature and concentration effects, *J Phys Chem B,* 110(2006)8856–8864.
8. Paolantoni M, Gallina M E, Sassi P, Morresi A, Structural properties of α-D-glucose solutions in dimethylsulphoxide probed by Raman spectroscopy, *J Chem Phys,* 130(2009)164501; doi.org/10.1063/1.3116250.
9. Auer B M, Skinner J L, IR and Raman spectra of liquid water: Theory and interpretation, *J Chem Phys*, 128(2008) 224511; doi.org/10.1063/1.2925258.
10. Hribar B, Southall N T, Vlachy V, Dill K A, How ions affect the structure of water, *J Am Chem Soc*, 124(2002)12302–12311.
11. Comez L, Paolantoni M, Sassi P, Corezzi S, Morresi A, Fioretto D, Molecular properties of aqueous solutions: a focus on the collective dynamics of hydration water, *Soft Matter*, 12(2016)5501–5514.
12. Fox M F, Hayon E, The Far-ultraviolet solution spectroscopy of chloride ion, *J Chem Soc*, *Faraday trans*, 86(1990) 257–263.
13. Elton D C, Fernàndez-Serra M., The hydrogen-bond network of water supports propagating optical phonon-like modes, *Nat Commun*, 7(2006)10193; doi.org/10.1038/ncomms10193.
14. Ashihara S, Fujioka S, Shibuya K, Temperature dependence of vibrational relaxation of the OH bending excitation in liquid H_2O, *Chem Phys Lett*, 502(2011)57–62.
15. Kanno H, Yonehama K, Somraj A, Yoshimura Y, Structure-making ions become structure breakers in glassy aqueous electrolyte solutions, *Chem Phys Lett*, 427(2006)82–86.
16. Wernersson E, Jungwirth P, Effect of Water Polarizability on the Properties of Solutions of Polyvalent Ions: Simulations of Aqueous Sodium Sulfate with Different Force Fields, *J Chem Theory Comput*, 6(2010)3233–3240.
17. Jungwirth P, Tobias D J, Specific Ion Effects at the Air/Water Interface*, Chem Rev*, 106(2006)1259–1281.
18. Vazdar M, Uhlig F, Jungwirth P, Like-Charge Ion Pairing in Water: An ab Initio Molecular Dynamics Study of Aqueous Guanidinium Cations, *J Phys Chem Lett*, 3(2012)2021–2024.
19. Tauber M J, Mathies R A, Structure of the Aqueous Solvated Electron from Resonance Raman Spectroscopy: Lessons from Isotopic Mixtures, *J Am Chem Soc*, 125(2003)1394–1402.
20. Eftekhari-Bafrooei A, Borguet E, Effect of Hydrogen-Bond Strength on the Vibrational Relaxation of Interfacial Water, *J Am Chem Soc*, 132(2010)3756– 3761.
21. Heisler I A, Meech S R, Low-Frequency Modes of Aqueous Alkali Halide Solutions: Glimpsing the Hydrogen Bonding Vibration, *Science*, 327(2010)857– 860.
22. Li R, Jiang Z, Guan Y, Yang H, Liu B, Effects of Metal Ion on the Water Structure Studied by the Raman O-H Stretching Spectrum, *J Raman Spectrosc*, 40(2009)1200–1204.
23. Smith J D, Saykally R J, Geissler P L, The Effects of Dissolved Halide Anions on Hydrogen Bonding in Liquid Water, *J Am Chem Soc*, 129(2007)13847–13856.
24. Bakker R J, Raman spectra of fluid and crystal mixtures in the systems H_2O, H_2O–NaCl and H_2O–$MgCl_2$ at low temperatures: applications to fluid-inclusion research, *The Canadian Mineralogist*, 42(2004)1283–1314.
25. Hanke F., Bottger U., Pavlov S. G., Hubers H. W., Raman Spectra of Frozen Salt Solutions Relevant for Planetary Surfaces, *EPSC Abstracts*, 9(2014)403-1.
26. Malley P P, Chakraborty S, Kahan T F, Physical characterization of frozen saltwater solutions using Raman microscopy, *ACS Earth and Space Chemistry*, 2(2018)702–710.
27. Nie G L, Sang S H, Cui R Z, Solid–Liquid Equilibrium Phase Diagram and Calculation in the Quaternary System (KBr+ NaBr+ $MgBr_2$+ H_2 O) at 298 K, *J Sol Chem*, 48(2019)862–874.

28. Perera P, Wyche M, Loethe Y, Ben-Amotz D, Solute-Induced Perturbations of Solvent-Shell Molecules Observed Using Multivariate Raman Curve Resolution, *J Am Chem Soc*, 130 (2008)4576–4577.
29. Wang S, Fang W, Li T, Li F, Sun C, Li Z, Men Z, An insight into liquid water networks through hydrogen bonding halide anion: Stimulated Raman scattering, *J Appl Phys*, 119(2016)163104; doi.org/10.1063/1.4947292.
30. Hu Q, Zhao H, Ouyang S, Interpreting the Raman OH/OD stretch band of ice from isotopic substitution and phase transition effects, *PhysChemChemPhys*, 20(2018)28600–28605.
31. Gallina M E, Sassi P, Paolantoni M, Morresi A, Cataliotti R S, Vibrational Analysis of Molecular Interactions in Aqueous Glucose Solutions. Temperature and Concentration Effects, *J Phys Chem B*, 110(2006)8856–8864.
32. Sun Q, Raman spectroscopic study of the effects of dissolved NaCl on water structure, *Vib Spectrosc*, 62(2012)110–114.
33. Busing W R, Hornig D F, The effect of dissolved KBr, KOH or HCl on the Raman spectrum of water, *J Phys Chem*, 65(1961)284–292.
34. Auer B M, Kumar R, Schmidt J R, Skinner J L, Hydrogen bonding and Raman, IR, and 2D-IR spectroscopy of dilute HOD in liquid D_2O, *PNAS*, 104(2007)14215–14220.
35. Hu Q, Zhao H, Ouyang S, Understanding water structure from Raman spectra of isotopic substitution H_2O/D_2O up to 573 K, *Phys Chem Chem Phys*, 19(2017)21540–21547.
36. Śmiechowski M, Janusz S, Vibrational spectroscopy of semiheavy water (HDO) as a probe of solute hydration, *Pure and Appl Chem,* 82(2010)1869–1887.
37. Bergmann U, Di Cicco A, Wernet P, Principi E, Glatzel P, Nilsson A, Nearest-neighbor oxygen distances in liquid water and ice observed by x-ray Raman based extended x-ray absorption fine structure, *J Chem Phys*, 127(2007) 174504; doi.org/10.1063/1.2784123.
38. Badger R M, Bauer S H, Spectroscopic studies of the hydrogen bond. II. The shift of the O–H vibrational frequency in the formation of the hydrogen bond, *J Chem Phys*, 5(1937)839–851.
39. Iogansen A V, Direct proportionality of the hydrogen bonding energy and the intensification of the stretching ν (XH) vibration in infrared spectra, *Spectrochim Acta* , 55A(1999)1585–1612.
40. Mikenda W, Steinböck S, Stretching frequency vs. bond distance correlation of hydrogen bonds in solid hydrates: A generalized correlation function, *J Mol Struct*, 384(1996)159–163.

[Received: 25.10.2021; accepted: 14.12.2021]

Letizia Scarabattoli received her Bachelor and Master degreee in Chemistry from the Department of Chemistry, Biology and Biotechnology of the University of Perugia in 2019 and 2021, respectively, working with Professor Paola Sassi. Her Bachelor and Master projects focused on studying systems (protein and electrolyte solutions) using vibrational spectroscopic techniques, in particular Raman and IR. She deepened her knowledge in the field of Raman spectroscopy during the internship carried out by the Erasmus+ project at the Department of Chemistry and Physics of Materials of the University of Salzburg.

Dr Lucia Comez has *Master's and Ph D degrees* in Physics. She was post-doc at the University of Perugia in the Physics Department and in 2002; became researcher at the Italian Institut of Matter Physics-National Research Council (INFM-CNR). Since 2008 she is a permanent researcher of the National Research Council at the Istituto Officina dei Materiali (CNR-IOM). From March 2016 to March 2020, she headed the UOS-IOM in Perugia.

Topical scientific interests include structural and dynamical studies of glasses, hydrogels, proteins, canonical and non-canonical DNA under different environmental conditions. She has a background as a spectroscopist, and she gained experience both in in-house techniques, Brillouin and Raman scattering, circular dichroism and UV-vis spectroscopy, and in large scale facilities around the world: ELETTRA (Italy), ESRF and ILL (France), ISIS (UK), MLZ (Germany), Spring-8 (Japan). She has co-published about 90 peer-reviewed papers and 2 book chapters. She presented several contributions to international conferences, and research centers. She is/ tutor for several (master degree and Ph D) students. She is a member of Società Italiana di Spettroscopia Neutronica (SISN), Consorzio Interuniversitario Nazionale per la Scienza e Tecnologia dei Materiali (INSTM), and European Molecular Liquids Group (EMLG).

Since 2014, she is in the board of the "Ph D Science and Tecnology for Physics and Geology School" at UNIPG, and in the same year become member of the Proposal Review Panel of the European Research Infrastructure Consortium (CERIC-ERIC). Since 2017, she is director of the biennial workshop/school "Frontiers in Water Biophysics" that takes place in Erice, Sicily (Italy), in the Ettore Majorana Foundation and Centre For Scientific Culture.

Dr Paola Sassi has a Master's degree in Chemistry and doctoral degree in Chemical Sciences. She is currently Associate Professor of Physical Chemistry at the University of Perugia in the Department of Chemistry Biology and Biotechnology. Dr Sassi has an extensive publication record of more than 120 manuscripts. She is author of more than 150 (oral and poster) contributions in national and international congresses. Over the course of her professional career, Dr Sassi has established a number of international collaborations and has trained numerous Ph D students and postdoctoral fellows in the aspects of molecular spectroscopy. As a researcher of physical chemistry, she deals with the spectroscopic characterization of biomaterials (cells and tissues), and the study of chemical-physical properties of liquids and macromolecules in solution. Vibrational, orientational and structural relaxation processes of simple and complex fluids are also studied by means of Raman, Depolarized Rayleigh and Brillouin scattering, together with FTIR absorption. Since January 2017, she is a member of the Proposal Review Panel of ELETTRA SINCROTRONE Trieste – Scattering beamline, and a member of the Proposal Review Panel of the European Research Infrastructure Consortium (CERIC-ERIC) – IUVS and SISSI beamlines.